SARCOIDOSIS VASCULITIS AND DIFFUSE LUNG DISEASES 2017; 34; 307-314

Contrast-enhanced cardiac Magnetic Resonance: distinction between cardiac sarcoidosis and infarction scar

Jan-Peter Smedema[1], Robert-Jan van Geuns[2], Rene Truter[4], Bongani M. Mayosi[3], Harry J.G.M Crijns[1]

[1] Departments of Cardiology, Maastricht University Medical Centre, The Netherlands; [2] Department of Cardiology and Radiology, Erasmus Medical Centre, Rotterdam, The Netherlands; [3] The Cardiac Clinic, Department of Medicine, Groote Schuur Hospital and University of Cape Town, Cape Town, South Africa; [4] Schnetler, Corbett and Associates, Panorama Medi-Clinic, Cape Town, South Africa

Abstract. *Objectives:* To review the value of delayed contrast-enhanced cardiac magnetic resonance (CECMR) in differentiating patients with cardiac sarcoidosis (CS) from those with coronary artery disease and recent myocardial infarctions. *Background:* Late gadolinium enhancement (LGE) accurately delineates myocardial necrosis or fibrosis. The pattern of LGE in ischemic and non-ischemic myocardial disease is different, and might be helpful in distinguishing CS from ischemic disease. *Methods:* The CECMR studies of 30 patients with CS were compared to those performed in 30 consecutive infarct patients, who had been managed with primary coronary interventions, and 10 healthy controls. Two experienced blinded observers classified patients by assessing the distribution of LGE. *Results:* LV LGE was present in 29/30 CS (mean 3.8 segments, range 0-12), all infarct (mean 4.3 segments, range 0-9), and none of the patients in the control group. The amount of LV LGE did not differ significantly between CS and infarct patients (19 ± 11% and 19 ± 12%, P= 0.8). The CS group exhibited a predominantly patchy, 3 layer LGE (P = 0.01), whereas confluent transmural LGE (P = 0.04) with a vascular distribution (P < 0.001) was prevalent in the infarct group. Significantly more RV LGE (P = 0.01) and dilation (P = 0.02) were found in the CS group. The two observers classified patients correctly as CS in 72% and 83% of cases, as ischemic in nature in 77% and 80% of cases, and as normal in 90% and 100% respectively. *Conclusions:* Gadolinium CMR was helpful in differentiating patients with CS from patients with ischemic heart disease and previous myocardial infarctions. In a subgroup of ischemic patients the pattern of LGE was atypical, and suggestive of non-ischemic etiology. *(Sarcoidosis Vasc Diffuse Lung Dis 2017; 34: 307-314)*

Key words: cardiac sarcoidosis, coronary artery disease, Magnetic Resonance Imaging, myocardial fibrosis

Abbreviations:

CECMR	= Contrast-Enhanced Cardiovascular Magnetic Resonance
CS	= cardiac sarcoidosis
IR-GRE	= inversion-recovery gradient echo
LV	= left ventricle
LGE	= late gadolinium enhancement
RV	= right ventricle

Received: 28 August 2016
Accepted after revision: 9 January 2017
Correspondence: Jan-Peter Smedema
Suite 2C5, Netcare Blaauwberg Hospital, Waterville Crescent, Sunningdale 7441, Cape Town, Republic of South Africa
Tel. 021-5543731 - Fax 021-5543741
E-mail: jansmedema@hotmail.com

Introduction

Sarcoidosis is a multi-system granulomatous disorder of unknown etiology with cardiac involvement in approximately twenty to thirty percent of patients (1). The clinical features of sarcoid heart disease include congestive heart failure, cor pulmonale, supraventricular and ventricular arrhythmias, atrioventricular and intraventricular conduction disease, ventricular aneurysms, pericardial effusion and sudden death (1). The diagnosis of cardiac sarcoidosis (CS) is made in the co-existence of non-caseating granulomas on myocardial biopsy or biopsies of any extracardiac tissue (with the exclusion of other causes for

granulomatous inflammation such as mycobacterial or fungal infection) and cardiovascular abnormalities for which other possible causes have been excluded (2). The value of gadolinium-enhanced cardiac magnetic resonance (CMR) in the diagnosis and management of this condition has been demonstrated (2-4). Late gadolinium enhancement (LGE) by CMR is the most accurate non-invasive method to evaluate myocardial necrosis or fibrosis caused by acute myocardial infarction, chronic myocardial infarction or non-ischemic myocardial disease (5). The distribution of LGE was valuable in differentiating between ischemic and non-ischemic myocardial scarring (6-9). Since a significant number of patients with CS present with symptoms of heart failure or chest pain, similar in nature to those in patients with coronary artery disease, we aimed to determine whether CMR, and specifically the pattern of MDE, would allow us to distinguish the CS patients from patients with coronary artery disease and recent myocardial infarcts.

Patients and methods

Patient population

Between July 1998 and November 2004 thirty patients were diagnosed with CS according to modified guidelines, based on the Study Report on Diffuse Pulmonary Diseases of the Japanese Ministry of Health and Welfare (1993) (2). We compared the CMR findings in the CS patients with those of 30 consecutive patients who had presented with myocardial infarcts, and who had CECMR studies during the study period. We included CECMR studies of 10 healthy control subjects. All patients in the infarct group had recently been diagnosed with myocardial infarction as defined by the European Society of Cardiology and American College of Cardiology, and underwent coronary angiography with (primary) percutaneous coronary interventions. (10) Twenty patients had myocardial infarction in the distribution of a single coronary artery (right coronary artery: 6 patients, left anterior descending artery: 7 patients, left circumflex artery: 7 patients), while ten patients had infarcts in the distribution of two coronary arteries (right coronary artery and left anterior descending artery: 4 patients, left anterior descending artery and left circumflex artery: 4 patients, right coronary artery and left circumflex artery: 2 patients). Since the study concerned retrospective analysis of clinical data in the CS and infarct groups, the Institutional Review Board waived the need for consent according to Dutch legislation. The Board approved the CMR studies in the control subjects, and all controls provided written informed consent.

CMR protocol

Studies were performed using a 1.5 Tesla MRI scanner [(Philips, Best, The Netherlands (53 patients), Siemens, Erlangen, Germany (3 patients, 10 controls) and General Electric, Milwaukee, Wisconsin, USA (4 patients)] with a cardiac-dedicated phased-array coil. The CMR studies were ECG triggered by standard software. All patients underwent steady-state-free precession studies of short axis, vertical long axis and four chamber views, to assess regional wall motion abnormalities. Before and ten minutes after the administration of 0.1 mmol/kg gadolinium-DTPA (Schering, Berlin), short axis, vertical long axis and 4 chamber images were obtained with Spin Echo in 5 patients (slice thickness 8 mm, gap .8 mm, matrix 512 × 512, FOV 380 mm, voxel size 0.7 mm × 0.7 mm × 8 mm), and 3-D breath hold inversion recovery-gradient echo (IR-GRE) sequences, obtained in diastole to minimize artifact due to cardiac motion, in the remaining 55 patients and 10 controls (slice thickness 10 mm, no gap, matrix 256 × 256, FOV 400 mm, voxel size 1.6 mm × 1.6 mm × 10 mm) to assess for the presence of LGE. The inversion time (250-400 msec) was determined on an individual basis to obtain optimal nulling of the unenhanced myocardial signal. The total time required for the investigation was 30-45 minutes.

CMR Analysis

CMR studies were analyzed off-line using commercially available software (CAAS MRV 3, Pie Medical Imaging, Maastricht, The Netherlands). Ventricular parameters were assessed in a standard way (11). Regional wall motion abnormalities, loss of wall thickness and left ventricular (LV) LGE were localized according to the standard 17 segment model (12). After delineating the endocardial and epicardial LV contours manually, the hyper-enhanced myocardium was depicted by changing the threshold setting for

signal intensity. Signal intensities of LV and right ventricular (RV) LGE, and remote unenhanced LV and RV myocardium were measured in the short axis slice with the highest level of enhancement. The cut off signal intensity value for LGE was two times the standard deviation of remote unenhanced myocardium. The absolute and relative amounts of LV LGE were computed by the post-processing software. RV LGE was considered to be present when seen in both the short axis and four chamber views. The distribution of LV LGE was classified as sub-endocardial, mid-wall, subepicardial, patchy three-layer involvement, or confluent transmural involvement. Two blinded, independent observers (RT, BMM) were asked to differentiate between the three groups based on the presence and distribution of LGE. To test for intraobserver variability, one observer (RT) repeated the assessment after a month, while blinded to previous results.

Statistical analysis

All statistical analyses were performed with a commercially available statistical software program (SSPS for Windows, version 21; SPSS, Chicago, Ill). Group data were expressed as mean ± SD. Continuous variables were assessed using the parametric *t* test for independent samples or Mann Whitney test where appropriate, and all categorical variables were assessed using the chi-square test. Statistical significance was defined as a p value less than 0.05. Bland-Altman analyses and intra-class correlation coefficients were used to determine intra-observer variability in the assessment of ventricular masses, volumes, ejection fractions, and the amount of LGE. We used kappa values to assess interobserver variability in determining the presence and localization of LGE, the diagnostic accuracy of the observers and the intra-observer variability in diagnosing CS and infarcts by LGE CMR.

Results

Patient characteristics

The demographic and background medical data are summarized in Table 1. The patients suffering

Table 1. Summary of demographic and background medical data

	Coronary Artery Disease (n = 30)	Cardiac Sarcoidosis (n = 30)	Controls (n = 10)	p value*
Mean age (years)	62 ± 13	49 ± 8	39 ± 14	**p < 0.001**
Sex (M/F)	27/3	19/11	9/1	**p = 0.02**
Body Surface Area (m^2)	1.93 ± 0.11	1.89 ± 0.19	1.89 ± 0.22	p = 0.3
Functional class				p = 0.2
NYHA I	10	14	10	
NYHA II	17	10	0	
NYHA III	3	4	0	
NYHA IV	0	2	0	
Angina	30	0	0	**p < 0.001**
Palpitations	4	19	0	**p < 0.001**
Syncope	2	4	0	p = 0.7
Hypertension	10	2	0	**p = 0.02**
Diabetes Mellitus	8	1	0	**p = 0.03**
12-lead ECG				
Atrial Fibrillation	0	0	0	
Bundle Branch Block	5	7	0	p = 0.5
RBBB	0	1	0	
LBBB	4	3	0	
LAHB	1	1	0	
Bifascicular block	0	2	0	
Atrio-ventricular Block	0	4	0	p = 0.1
Grade II AV Block	0	2	0	
Grade III AV Block	0	2	0	
Q wave	11	2	0	**p = 0.01**

* P values concern the comparison between he groups with coronary artery disease and cardiac sarcoidosis

Table 2. Summary of the findings with gadolinium-enhanced cardiac magnetic resonance

	Coronary Artery Disease (n = 30)	Cardiac Sarcoidosis (n = 30)	Controls (n = 10)	P value*
Left Ventricular mass (gram)	122 ± 28	129 ± 61	97 ± 40	p = 0.6
Left Ventricular mass index (gram/m²)	64 ± 16	68 ± 26	51 ± 18	p = 0.5
Left Ventricular Hypertrophy (pts)	4 (13%)	7 (23%)	0	p = 0.5
Regional LGE (pts)	30 (100%)	29 (97%)	0	p = 1.0
Number of Left Ventricular segments with LGE	127/510 (25%)	117/510 (23%)	0	p = 0.4
Range per patient	0 - 9	0-12		
Mean	4.3	3.8		
Sub-endocardial LGE (pts)	6 (20%)	5 (17%)	0	p = 1.0
Confluent, coronary artery distribution	6 (20%)	0		**p = 0.02**
Patchy	0	5 (17%)		**p = 0.01**
Sub-endocardial + Mid-wall LGE (pts)	5 (17%)	1 (3%)	0	p = 0.2
Mid-wall MDE (pts)	0	2 (7%)	0	p = 0.5
Sub-epicardial + Mid-wall LGE (pts)	2 (7%)	0	0	p = 0.5
Patchy LGE of all 3 Left Ventricular layers (pts)	9 (30%)	19 (63%)	0	**p = 0.01**
Transmural confluent Left Ventricular LGE (pts)	8 (27%)	2 (7%)	0	**p = 0.04**
One focus of LGE (pts)	21	10	0	**p = 0.02**
Multiple foci of LGE (pts)	9	19	0	**p = 0.02**
Vascular segmental distribution of LGE (pts)	25	3	0	**p < 0.001**
Left Ventricular LGE (gram)			0	p = 0.8
Min - Max	7 - 68	0 -73		
Mean	26 ± 14	27 ± 21		
Left Ventricular LGE (%)				p = 0.8
Min - Max	6 - 47	0 - 38		
Mean	19 ± 11	19 ± 12		
Left Ventricular End-Diastolic Volume (ml)				p = 0.08
Min - Max	103 - 573	74 - 308	107 - 229	
Mean ± SD	194 ± 84	160 ± 58	154 ± 33	
Left Ventricular End-Diastolic Volume index (ml/m²)				**p = 0.01**
Min - Max	57 - 311	36 - 148	64 - 102	
Mean ± SD	101 ± 47	75 ± 29	81 ± 101	
Left Ventricular Ejection Fraction (%)				**p = 0.005**
Min - Max	6 - 63	21 - 70	52 - 73	
Mean ± SD	37 ± 14	49 ± 14	62 ± 6	
Dilated Left Ventricle (pts)	15 (50%)	9 (30%)	1 (10%)	p = 0.1
Left Ventricular Ejection Fraction < 55% (pts)	25 (83%)	17 (57%)	1 (10%)	**p = 0.047**
Loss of Left Ventricular wall thickness (pts)	20 (67%)	9 (30%)	0	**p = 0.009**
Left Ventricular wall motion abnormalities (pts)	23 (77%)	12 (40%)	0	**p = 0.008**
Right Ventricular LGE (pts)	3 (7%)	8 (27%)	0	**p = 0.01**
Dilated Right Ventricle (pts)	2 (7%)	10 (33%)	0	**p = 0.02**
Right Ventricular Ejection Fraction < 45% (pts)	19 (63%)	12 (40%)	1 (10%)	p = 0.1
Right Ventricular End-Diastolic Volume (ml)				P = 0.7
Min - Max	94 - 258	79 - 260	94 - 169	
Mean ± SD	162 ± 38	157 ± 48	123 ± 28	
Right Ventricular End-Diastolic Volume index (ml/m²)				p = 0.9
Min - Max	53 - 147	40 - 138	55 - 87	
Mean ± SD	85 ± 20	85 ± 26	65 ± 10	
Right Ventricular Ejection Fraction (%)				p = 0.5
Min - Max	15 - 60	18 - 64	46 - 69	
Mean ± SD	43 ± 12	46 ± 12	58 ± 6	

* P values concern the comparison between he groups with coronary artery disease and cardiac sarcoidosis
LGE = myocardial delayed enhancement

from coronary artery disease were significantly older, had more cardiovascular risk factors, and pathological Q-waves on their 12-lead ECG's.

Cardiac Magnetic Resonance

The CMR findings are summarized in Table 2. The LV ejection fraction and LV end-diastolic volume index differed significantly between the CS and infarct groups, with more loss of regional LV wall thickness (P = 0.009) and wall motion abnormalities (P = 0.008) resulting in poorer systolic function (P = 0.047) and larger ventricles (P = 0.01) in the latter group. LGE of the LV was present in 29/30 CS patients (mean 3.8 segments/patient, range 0-12), 30/30 infarct patients (mean 4.3 segments/patient, range 0-9), and none of the control group. The amount of LGE did not significantly differ between the CS and infarct groups (P = 0.8). Most enhancing lesions in the CS group were located in the basal and anterolateral LV (segments 1-6, 12 and 16; 74 out of 117 enhancing segments (64%), compared to 58/127 (46%) for the MI group). In the majority of CS patients (19/30, 63%) patchy LGE involved all three myocardial layers. In 2/30 (7%) confluent transmural LGE was present, suggesting co-existing coronary artery disease (Figure 1A). But coronary angiography showed unobstructed epicardial coronary arteries. In 25/30 (83%) patients of the infarct group the distribution of LGE was suggestive of underlying coronary artery disease, since hyper-enhancement started at the subendocardium and involved segments restricted to the vascular territory of specific coronary arteries. Sole mid-layer involvement was only seen in patients with CS, while LGE involving both the subendocardial and mid myocardial layers was predominantly seen in infarct patients. When considering sole mid layer, patchy subendocardial and three layer LGE to be diagnostic of CS, 26/30 (87%) would have been correctly classified (Figure 2A, C, E). Significantly more RV LGE (8 (27%) versus 3 (7%) patients, P = 0.01) and RV dilation (10 (33%) versus 2 (7%) patients, P = 0.02) was found in the CS group (Figure 3). The observers correctly diagnosed CS in 21/29 (72%), 24/29 (83%), 21/29 (72%), ischemic heart disease in 23/30 (77%), 23/30 (77%), 24/30 (80%) and normal controls in 9/10 (90%), 10/10 (100%), 10/10 (100%). The kappa values for interobserver agreement in differentiating between CS, infarcts and normal controls by assessing the LGE CMR studies were 0.91 (0.86, 0.95), and 0.86 (0.81, 0.92). The kappa value for intra-observer agreement in differentiating between CS, infarcts and normal controls by assessing the LGE CMR studies was 0.86 (0.81, 0.92). There was excellent intra- and interobserver correlation for ventricular volumes, masses, and ejection fractions. The intraclass correlation coefficient for LV LGE was 0.989 [0.981-0.993] (p=0.001).

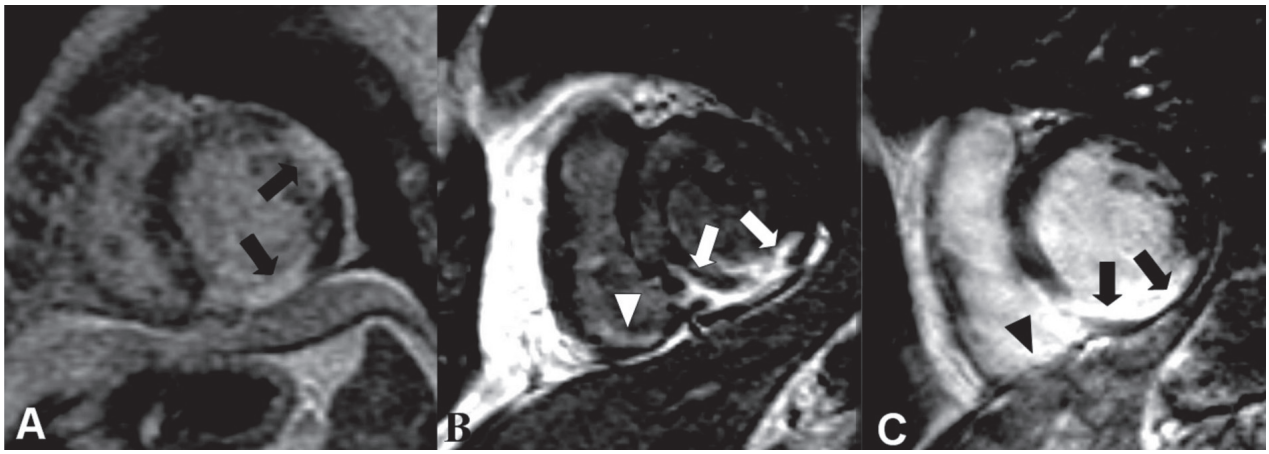

Fig. 1. Delayed-enhanced three-dimensional breath-hold inversion-recovery gradient echo studies (short axis views) demonstrating multifocal transmural hyper-enhancement involving the inferior and lateral LV segments in a patient with sarcoidosis (A), and patchy (B) respectively confluent (C) transmural inferior LV (arrows) and RV (arrowheads) wall late gadolinium enhancement secondary to infarctions in patients with coronary artery disease of the RCA

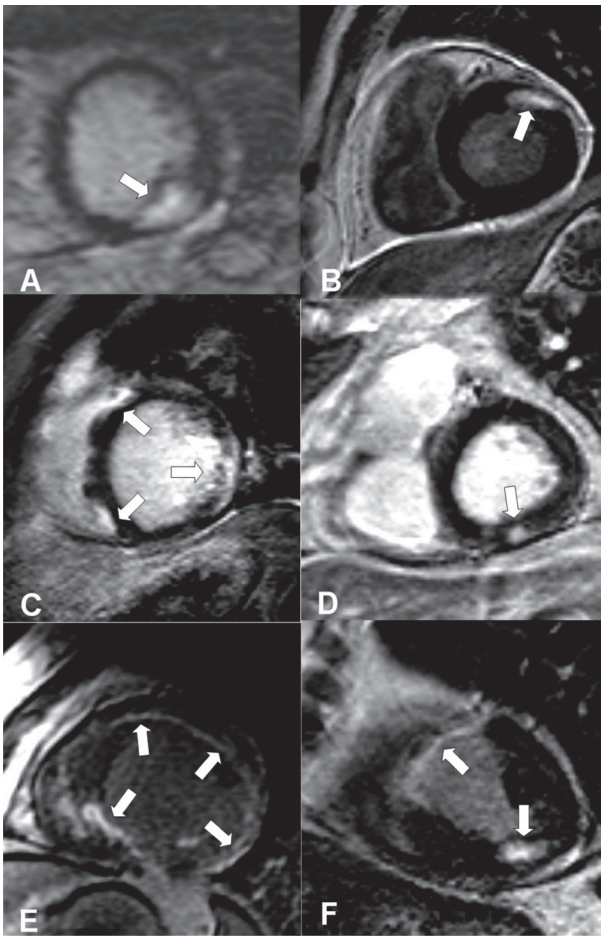

Fig. 2. Delayed-enhanced three-dimensional breath-hold inversion-recovery gradient echo studies (short axis views) of three patients with cardiac sarcoidosis, demonstrating: focal (A) and patchy, multi-segmental three layer hyper-enhancement (C and E), and three patients with coronary artery disease demonstrating: focal sub-epicardial infarctions in the distribution of respectively the LCX (B) and RCA (D), and two-vessel disease (F) involving the LAD (subendocardial infarction) and RCA (mid-layer infarction)

Discussion

Our study is the first to systematically compare the distribution of LGE in CS with the findings in patients with coronary artery disease. Our findings suggest that CECMR is helpful in the non-invasive differentiation between patients with CS and patients with coronary artery disease and previous myocardial infarcts. However, in approximately a third of patients with coronary artery disease, subepicardial or patchy, three layer LGE was found, a pattern that was suggestive of a non-ischemic etiology such as

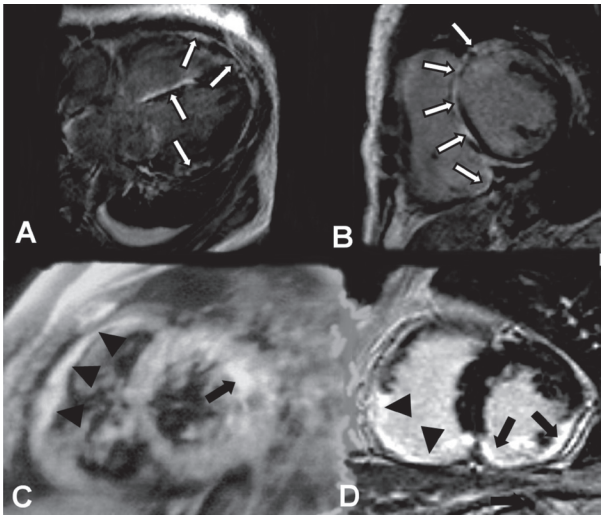

Fig. 3. Delayed-enhanced three-dimensional breath-hold inversion-recovery gradient echo studies (A: 4 chamber view; B, D: short axis views) demonstrating multi-segmental, patchy three layer hyper-enhancement in a patients with sarcoidosis (A,B) and confluent transmural hyper-enhancement in the vascular distribution of the RCA (D). The delayed-enhanced spin echo study (C: short axis view) shows patchy, three layer involvement of the lateral LV segments. Transmural right ventricular enhancement secondary to sarcoidosis (C) and coronary artery disease (D) is demonstrated by the arrowheads

CS (6-8). Additional angiographic information was needed to correctly classify 11 patients with coronary artery disease and 3 with CS.

LGE results from the sustained presence of gadolinium in the myocardium, secondary to expansion of the interstitial space or impaired microvascular wash out ("no-reflow phenomena"), and has been reported in a variety of conditions, such as coronary artery disease, cardiomyopathies, myocarditis, and myocardial infiltration, that are characterized by necrosis, fibrosis or inflammation (2-9). In CS the presence of active, granulomatous inflammation and the resulting myocardial fibrosis are considered to be the underlying histopathological substrate resulting in the accumulation of gadolinium (2-4). Recent studies have determined subendocardial and transmural LGE to be diagnostic of underlying coronary artery disease, while sole mid-layer and epicardial LGE were predominantly seen in patients with non-ischemic cardiomyopathies (2-9). Although sole subepicardial myocardial fibrosis is considered rare in coronary artery disease, both our patients with epicardial LGE happened to be infarct patients (13) (Figure 3). Early presentation and primary percu-

taneous interventions may have resulted in smaller, myocardial scars with an atypical mural distribution (14) (Figure 2B, D, F, 4B, D).

The pattern of LGE in CS has been reported to be patchy, multi-segmental, not related to coronary artery territories, while predominantly involving the mid myocardial and subepicardial layers (2-4). When considering sole mid-layer, and patchy subendocardial or patchy transmural LGE to be diagnostic of CS, and confluent subendocardial or confluent transmural LGE diagnostic of coronary artery disease, the sensitivity, specificity and overall accuracy of LGE CMR for these conditions respectively would be 87%, 70%, 78%, and 63%, 90% and 77%. The significantly higher number of patients with loss of regional wall thickness, wall motion abnormalities, and generally poorer systolic LV function in the infarct group is explained by more extensive, confluent, transmural LGE in this group (15).

RV LGE and dilation was present in a substantial number of CS patients. These findings may be explained by primary RV myocardial involvement, but alternatively the presence of pulmonary arterial hypertension, resulting from extensive pulmonary sarcoidosis, has been considered a possible cause of RV fibrosis (16). The junction of right and left ventricle and right-sided interventricular septum seemed to be predominantly affected (Figure 4). However, further studies are needed to elucidate the underlying mechanisms and significance of RV LGE in patients with sarcoidosis. The absense of LGE in one patients with CS, with a dilated, globally hypokinetic LV, may be explained by the presence of diffuse myocardial fibrosis, which is not detected with the IR-GRE technique.

IR-GRE is the current gold standard technique in the assessment of myocardial fibrosis, and we may have underestimated the amount of myocardial scar tissue by relying on Spin Echo sequences in 5 patients. The distribution of LGE in these particular patients was however strongly suggestive of CS, in that it concerned patchy subendocardial or three layer hyperenhancement. Since the majority of patients were not assessed with first-pass myocardial perfusion studies, we did not include these data. The presence of flow limiting coronary artery disease in the infarct group might have improved the diagnostic accuracy of CMR in this group.

In conclusion, the presence of sole mid-layer, and patchy, subendocardial or three layer LGE with a non-vascular distribution, in patients with extracardiac sarcoidosis suggests cardiac involvement, and differentiates these patients from patients with coronary artery disease.

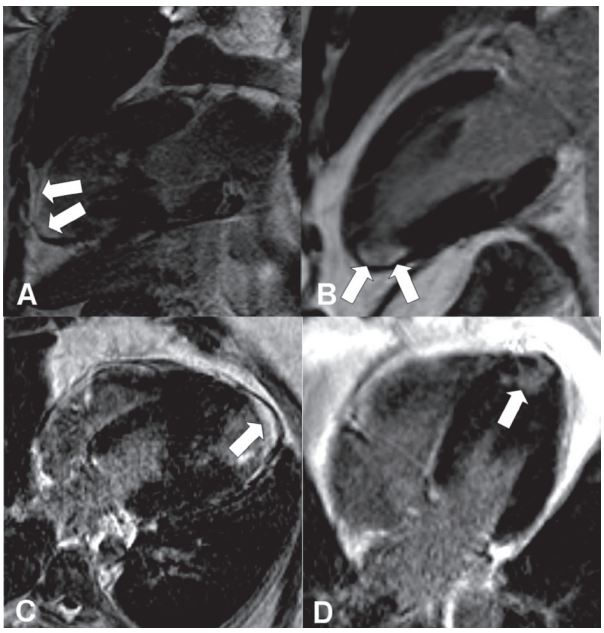

Fig. 4. Delayed-enhanced three-dimensional breath-hold inversion-recovery gradient echo studies demonstrating confluent apical hyper-enhancement secondary to sarcoidosis (A: vertical long axis view, C: 4 chamber view) and apical patchy three-layer hyperenhancement in a patient with coronary artery disease and myocardial infarction secondary to obstruction of the LAD (B: vertical long axis view, D: 4 chamber view)

References

1. Kim JS, Judson MA, Donnino R, et al. Cardiac sarcoidosis. Am Heart J 2009; 157(1): 9-21.
2. Smedema JP, Snoep G, van Kroonenburgh MJPG, et al. Evaluation of the diagnostic accuracy of gadolinium CMR in cardiac sarcoidosis. J Am Coll Cardiol 2005; 45: 1683-90.
3. Vignaux O, Dhôte R, Duboc D, et al. Clinical significance of myocardial magnetic resonance abnormalities in patients with sarcoidosis. A 1-year follow-up study. Chest 2002; 122: 1895-1901.
4. Vignaux O, Dhôte R, Duboc D, et al. Detection of myocardial involvement in patients with sarcoidosis applying T2-weighted, contrast-enhanced and cine magnetic resonance imaging: initial results of a prospective study. J Comput Assist Tomograph 2002; 26: 762-7.
5. Pennell DJ, Sechtem UP, Higgins CB, et al. Special article. Clinical indications for cardiovascular magnetic resonance (CMR): Consensus Panel report. European Heart Journal 2004; 25: 1940-65.
6. Hunold P, Schlosser T, Vogt FM, et al. Myocardial late enhancement in contrast-enhanced cardiac MRI: distinction between infarction scar and non-infarction-related disease. Am J Roentgenol 2005; 184(5): 1420-6.
7. Lim RP, Srichai MB, Lee VS. Non-Ischemic Causes of delayed my-

ocardial hyper-enhancement on MRI. Am J Roentgenol 2007; 188: 1675-81.
8. Mahrholdt H, Wagner A, Judd RM, Sechtem U, Kim RJ. Delayed enhancement cardiovascular magnetic resonance assessment of non-ischemic cardiomyopathies. Eur Heart J 2005; 26: 1461-74.
9. Laissy JP, Hyafil F, Feldman LJ, et al. M. Differentiating acute myocardial infarction from myocarditis: diagnostic value of early- and delayed-perfusion cardiac MR imaging. Radiology 2005; 237: 75-82.
10. Myocardial infarction redefined – A consensus document of the joint European Society of Cardiology/American College of Cardiology Committee for the Redefinition of Myocardial Infarction. J Am Coll Cardiol 2000; 36: 959-69.
11. Bellenger NG, Pennell DJ. Ventricular function. In: Manning WJ, Pennell DJ, eds. Cardiovascular Magnetic Resonance. New York, NY: Churchill Livingstone; 2002.
12. Cerqueira MD, Weissman NJ, Dilsizian V, et al. AHA writing group on myocardial segmentation and registration for cardiac imaging. Standardized myocardial segmentation and nomenclature for tomographic imaging of the heart. Circulation 2002; 105: 539-42.
13. Shirani J, Roberts WC. Subepicardial myocardial lesions. Am Heart J 1993; 125: 1346-52.
14. Ricciardi MJ, Wu E, Davidson CJ, et al. Visualization of discrete microinfarction after percutaneous coronary intervention associated with mild creatine kinase-MB elevation. Circulation 2005; 111: 1027-32.
15. Kim RJ, Wu E, Rafael A, et al. The use of contrast-enhanced magnetic resonance imaging to identify reversible myocardial dysfunction. N Engl J Med 2000; 343: 1445-53.
16. McCann GP, Gan CT, Beek Am, et al. Extent of MRI Delayed Enhancement of Myocardial Mass Is Related to Right Ventricular Dysfunction in Pulmonary Artery Hypertension. AJR 2007; 188: 349-55.